Lower tensor-to-scalar ratio as possible signature of modified gravity

Abraão J. S. Capistrano [*]
Universidade Federal do Paraná, Departmento de Engenharia e Exatas, Rua Pioneiro, 2153, Palotina, 85950-000, Paraná/PR, Brasil and Federal University of Latin American Integration (UNILA), Applied physics graduation program, Avenida Tarquínio Joslin dos Santos, 1000-Polo Universitário, Foz do Iguaçu, 85867-670, Paraná/PR, Brasil

Rafael C. Nunes [†]
Universidade Federal do Rio Grande do Sul, Instituto de Física, Porto Alegre, 91501-970, Rio Grande do Sul/RS, Brasil and Instituto Nacional de Pesquisas Espaciais, Divisão de Astrofísica, Avenida dos Astronautas 1758, São José dos Campos, 12227-010, São Paulo/SP, Brasil

Luís A. Cabral [‡]
Universidade Federal do Norte do Tocantins, Araguaína, 77824-838, Tocantins/TO, Brasil

(Received 21 March 2024; accepted 6 May 2024; published 10 June 2024)

This paper simplifies the induced four-dimensional gravitational equations originating from a five-dimensional bulk within the framework of Nash's embeddings, incorporating them into a well-known $\mu - \Sigma$ modified gravity parametrization. By leveraging data from *Planck* Public Release 4, BICEP/Keck Array 2018, *Planck* cosmic microwave background lensing, and baryon acoustic oscillation observations, we establish a stringent lower limit for the tensor-to-scalar ratio parameter: $r < 0.0303$ at a confidence level (CL) of 95%. This finding suggests the presence of extrinsic dynamics influencing standard four-dimensional cosmology. Notably, this limit surpasses those typically obtained through Bayesian analysis using Markov chain Monte Carlo techniques, which yield $r < 0.038$, or through the frequentist profile likelihood method, which yields $r < 0.037$ at 95% CL.

DOI: 10.1103/PhysRevD.109.123517

I. INTRODUCTION

Inflation has become one of the cornerstones of modern cosmology. It not only solves the flatness and horizon problems, but also describes the quantum seeds of cosmological fluctuations that eventually drove the Universe to evolve [1–9] throughout a brief and rapid period of exponential expansion right after the big bang. This inflationary period is thought to have smoothed out the early Universe's irregularities and laid the foundation for the large-scale structure we observe today. It is reinforced by the anisotropy seen in cosmic microwave background (CMB) observations [10]. While the precise mechanisms fueling inflation remain elusive, numerous competing theoretical models have emerged [11–21], each vying to explain this fundamental cosmic process. However, despite the ongoing debate, the overarching framework consistently yields predictions that align remarkably well with cosmological observations (see [22,23] for a review).

A significant portion of scientific inquiry into the origins of the Universe revolves around scrutinizing and characterizing the statistical properties of primordial density perturbations, particularly through the analysis of the statistical two-point function. Empirical evidence suggests that these fluctuations adhere closely to a Gaussian distribution and exhibit near scale invariance. Consequently, we can effectively capture their statistical behavior using a power-law power spectrum governed by two crucial parameters. These parameters, integral to the ΛCDM standard cosmological model, are the scalar amplitude A_s, representing the perturbation amplitude, and the spectral tilt n_s, governing the scale dependency of the density perturbation power spectrum. Remarkably, even with just these two parameters, we can glean insights into certain facets of inflationary dynamics today, shedding light on the energy scales pivotal during the early epochs of the Universe's evolution. Statistical analyses from canonical inflationary models constrain $n_s = 0.9649 \pm 0.0042$ and $\ln(10^{10} A_s) = 3.044 \pm 0.014$ at the 68% confidence level (CL) using *Planck*-CMB data [24]. Conversely,

[*] capistrano@ufpr.br
[†] rafadcnunes@gmail.com
[‡] cabral@uft.edu.br

analysis from ACT-CMB indicates agreement with a Harrison-Zel'dovich primordial spectrum, where $n_s = 1.009 \pm 0.015$ [25]. This introduces tension with *Planck*-CMB measurements. For further discussions on this topic, see also [26–28].

Another pivotal parameter arising from inflationary theories is the tensor-to-scalar ratio r, indicative of primordial gravitational waves. Multiple CMB experiments have already imposed stringent upper bounds on the amplitude of the tensor spectrum. Notably, the BICEP/Keck Collaboration has established the most stringent constraint to date, setting $r < 0.036$ at a 95% CL [29], effectively challenging certain classes of single-field monomial models. A frequentist profile likelihood method [30] was also used to investigate the discrepancy with Bayesian analysis using Markov chain Monte Carlo methods, identified by the SPIDER Collaboration [31]. As a result, they found an upper limit of $r < 0.037$ at 95% CL.

In this paper, we propose the possibility that the extrinsic curvature, which is thought of as the orthogonal component of the gravitational field besides the metric $g_{\mu\nu}$, works as an inflaton field. Differently from traditional extra-dimensional braneworld models [32–35], the dynamics of extrinsic curvature is considered. We focus on how a dynamic embedding should affect the physical Universe and may provide new insights on the current problems in cosmology. As a main character in this framework, the extrinsic curvature should not be restricted to the analysis of the background geometry but should also include its perturbative dynamics [36–38]. To do so, we start from the perturbations of the geometry adopting Nash-Greene theorem [39,40] which provides a general structure for embedding between non-Riemannian geometries [41–50]. This is rather different from common approaches of braneworld perturbative models in which the perturbations are triggered from confined sources. Then, the dynamics of the extrinsic curvature itself is replaced. A common practice in these models is to rely on junction conditions such as the Israel-Darmois-Lanczos (IDL) condition [51]. Commonly used in Randall-Sundrum models [33,34], the IDL condition replaces the extrinsic curvature by an algebraic relation with the energy-momentum tensor. It was shown that it belongs to a very special case [38,42] and, in general, can be completely removed or replaced [52].

The paper is organized as follows. Section II describes the essentials of embeddings as a mathematical background and summarizes our cosmological model with both background and perturbed cosmological equations. Moreover, the effective fluid approach is presented to develop a more realistic model to compare with observations. In Sec. III we present a simpler version of the model in the form of a modified gravity (MG) framework. Section IV is devoted to the analysis of extrinsic curvature as an inflaton field, in which we investigate the slow-roll conditions for the extrinsic potential. In Secs. V and IV we examine the model in contrast with cosmological data from the latest NPIPE *Planck* DR4 likelihoods [53,54], the BICEP2/Keck Collaboration [55], and a junction of the large-scale structure (LSS) catalog with the 6dF Galaxy Survey [56], the Seventh Data Release of the SDSS Main Galaxy Sample (SDSS DR7 MGS) [57], and clustering measurements of the Extended Baryon Oscillation Spectroscopic Survey (eBOSS) associated with the SDSS's Sixteenth Data Release [58]. The related joint likelihood analysis is computed with an MGCAMB-II [59] patch by means of a Cobaya [60] sampler. In Sec. VI we conclude with our remarks and prospects.

II. EMBEDDINGS AS A THEORETICAL BACKGROUND

We present the main results from previous works [41–44,49]. Once a general arbitrary D-dimensional case is possible [41,42], for comparison purposes with the recent literature, we define our model in five dimensions with a five-dimensional bulk V_5 and an embedded four-dimensional geometry V_4.

A gravitational action S is defined as

$$S = -\frac{1}{2\kappa_5^2}\int \sqrt{|\mathcal{G}|}{}^5\mathcal{R}d^5x - \int \sqrt{|\mathcal{G}|}\mathcal{L}^*_m d^5x, \tag{1}$$

where κ_5^2 is a fundamental energy scale on the embedded space, the curly ${}^5\mathcal{R}$ curvature means the five-dimensional Ricci scalar, and the matter Lagrangian $\mathcal{L}^*_m$ denotes the confined matter fields on a four-dimensional embedded space-time.

The nonperturbed extrinsic curvature $\bar{k}_{\mu\nu}$ is defined as [61]

$$\bar{k}_{\mu\nu} = -\mathcal{X}^A_{,\mu}\bar{\eta}^B_{,\nu}\mathcal{G}_{AB}, \tag{2}$$

where Eq. (2) shows the projection of the variation of the set of normal unitary vectors $\bar{\eta}^B$ onto the tangent plane orthogonal to the embedded space V_4. In other words, the variation of $\bar{\eta}^B$ leads to the bending of V_4 and its tangent components have coefficients $\bar{k}_{\mu\nu}$. The embedding coordinate $\mathcal{X}$ defines a regular local map $\mathcal{X}: V_4 \to V_5$ and must satisfy the embedding equations

$$\mathcal{X}^A_{,\mu}\mathcal{X}^B_{,\nu}\mathcal{G}_{AB} = g_{\mu\nu}, \qquad \mathcal{X}^A_{,\mu}\bar{\eta}^B\mathcal{G}_{AB} = 0, \qquad \bar{\eta}^A\bar{\eta}^B\mathcal{G}_{AB} = 1, \tag{3}$$

where $\mathcal{G}_{AB}$ denotes the metric components of the bulk V_5 in arbitrary coordinates. The embedding frame is defined by the set of coordinates $\{\mathcal{X}^A, \bar{\eta}^A\}$ that composes a Gaussian reference frame. Throughout the paper, except when explicitly stated otherwise, the overbar indicates a background (nonperturbed) quantity.

The bulk metric $\mathcal{G}_{AB}$ is defined as

$$\mathcal{G}_{AB} = \begin{pmatrix} g_{\mu\nu} & 0 \\ 0 & 1 \end{pmatrix}. \tag{4}$$

Concerning notation, uppercase Latin indices run from 1 to 5. Lowercase Latin indices refer to the one extra dimension considered. All greek indices refer to the embedded space-time counting from 1 to 4.

In this paper, we use the Nash theorem of 1956 [39]. The seminal result of this theorem shows how to produce orthogonal perturbations from the background metric $\bar{g}_{\mu\nu}$ given by

$$\bar{k}_{\mu\nu} = -\frac{1}{2}\frac{\partial \bar{g}_{\mu\nu}}{\partial y}, \tag{5}$$

where y is an arbitrary spatial coordinate along the orthogonal direction to the tangent plane. This mechanism avoids false perturbations due to the possibility of inducing coordinate gauges. Therefore, the physical effects of the extrinsic curvature associated with Eq. (5) represent an acceleration tangent to the four-dimensional space-time that always points to the concave side of the curve. As a result, it induces a Riemann stretching on the space-time geometry, which may be related to the accelerated expansion of the Universe [42,44].

As a consequence of Eq. (5), we have new geometries $g_{\mu\nu}$ generated from small perturbations on the background metric increments $\delta g_{\mu\nu}$ as

$$g_{\mu\nu} = \bar{g}_{\mu\nu} + \delta g_{\mu\nu}. \tag{6}$$

Moreover, one obtains the perturbed extrinsic curvature $k_{\mu\nu}$ as

$$k_{\mu\nu} = \bar{k}_{\mu\nu} + \delta k_{\mu\nu}, \tag{7}$$

where $\delta k_{\mu\nu} = -2\delta y\, g^{\sigma\rho} k_{\mu\sigma} k_{\nu\rho}$. In principle, this is a continuous process to any arbitrary perturbation increments of superior orders of $\delta g_{\mu\nu}$ and $\delta k_{\mu\nu}$. For our purposes, we keep the perturbations at linear order, as shown in Eqs. (6) and (7).

The increments $\delta g_{\mu\nu}$ and $\delta k_{\mu\nu}$ are the Nash fluctuations, which were later applied to non-Riemannian metrics by Greene [40]. The deformation formula in Eq. (5) is also a pivot element to obtain solutions of the Gauss and Codazzi equations

$${}^5\mathcal{R}_{ABCD}\mathcal{Z}^A_{,\alpha}\mathcal{Z}^B_{,\beta}\mathcal{Z}^C_{,\gamma}\mathcal{Z}^D_{,\delta} = \bar{R}_{\alpha\beta\gamma\delta} + (\bar{k}_{\alpha\gamma}\bar{k}_{\beta\delta} - \bar{k}_{\alpha\delta}\bar{k}_{\beta\gamma}), \tag{8}$$

$${}^5\mathcal{R}_{ABCD}\mathcal{Z}^A_{,\alpha}\mathcal{Z}^B_{,\beta}\mathcal{Z}^C_{,\gamma}\eta^D = \bar{k}_{\alpha[\beta;\gamma]}, \tag{9}$$

where ${}^5\mathcal{R}_{ABCD}$ is the five-dimensional Riemann tensor and $\bar{R}_{\alpha\beta\gamma\delta}$ is the background four-dimensional Riemann tensor. The perturbed embedding coordinate $\mathcal{Z}^A_{,\mu}$ is defined as $\mathcal{Z}^A_{,\mu} = \mathcal{X}^A_{,\mu} + \delta y \eta^A_{,\mu}$. The normal vector η^A is invariant under perturbations, i.e., $\eta^A = \bar{\eta}^A$. The semicolon in Eq. (9) denotes a covariant derivative with respect to the metric and the brackets apply the covariant derivatives to the adjoining indices. In Eq. (8), the Gauss equation entwines the bulk Riemann curvature as a reference point for the Riemann curvature of the embedded space-time. This relation is complemented by the Codazzi equation in Eq. (9), which shows the projection of the Riemann tensor of the bulk space along the orthogonal direction, resulting in the variation of the extrinsic curvature.

In order to guarantee the possibility to generate new geometries, in five dimensions, the set of coordinates $\mathcal{Z}^A$ also needs to satisfy embedding equations similar to Eq. (3),

$$\mathcal{Z}^A{}_{,\mu}\mathcal{Z}^B{}_{,\nu}\mathcal{G}_{AB} = g_{\mu\nu}, \qquad \mathcal{Z}^A{}_{,\mu}\eta^B\mathcal{G}_{AB} = 0, \qquad \eta^A\eta^B\mathcal{G}_{AB} = 1. \tag{10}$$

Then, Eqs. (6) and (7) are valid.

Like Kaluza-Klein and braneworld models, we consider that the dynamics of the bulk V_5 is governed by the higher-dimensional Einstein equations,

$${}^5\mathcal{R}_{AB} - \frac{1}{2}5\mathcal{R}\mathcal{G}_{AB} = G_* T^*_{AB}, \tag{11}$$

where G_* is the new gravitational constant and T^*_{AB} denotes the components of the energy-momentum tensor of the material sources. Those sources are confined to four dimensions, which is a consequence of the isomorphism between the three-form (from the derivative of the Yang-Mills curvature) and one-form current. This is valid only in four dimensions. Thus, all known observable sources of gravitation composing the generic energy-momentum tensor T^*_{AB} are also confined. This outcome is independent of the variation of the extra coordinate y. In other words, the four-dimensionality of space-time is a consequence of the invariance of the Maxwell equations under the Poincaré group. It is well known that any gauge theory can be mathematically constructed or extended in a higher-dimensional space, but in the present framework, the four-dimensionality of the embedded space-time will suffice based on what high-energy tests suggest [62–64]. Moreover, in the Gaussian frame $\{\mathcal{Z}^A, \eta^A\}$ of any perturbed space-time, we can write the confinement condition of the energy-momentum tensor source T^*_{AB} of the bulk Einstein equation in Eq. (11) with the projections

$$8\pi G T_{\mu\nu} = G_*\mathcal{Z}^A_{,\mu}\mathcal{Z}^B_{,\nu}T^*_{AB}, \quad \mathcal{Z}^A_{,\mu}\eta^B T^*_{AB} = 0, \quad \eta^A\eta^B T^*_{AB} = 0. \tag{12}$$

In this framework, the matter content is localized in the V_4 embedded space due to the fact that the Nash deformation formula in Eq. (5) imposes a geometric constraint on the confined sources. Any deformation is not arbitrary and can be generated by smooth perturbations along the direction δy orthogonal to the embedded space V_4. In five dimensions, this process is simplified and just one deformation parameter suffices to locally deform the embedded background. In general, the curvature radii l^a of the embedded background correspond to the direction in which the embedded space-time deviates more sharply from the tangent plane and are the solutions of the homogeneous equation

$$\det(g_{\mu\nu} - l^a k_{\mu\nu a}) = 0. \quad (13)$$

This is a local invariant property of the embedded space-time and does not depend on the chosen Gaussian system. The smallest solution l provides

$$\frac{1}{l} = (g_{\mu\nu}\mathcal{G}^{AB} l^\mu_A l^\nu_B)^{-1/2}. \quad (14)$$

In other words, l constrains a local limit for the region in which the bulk is accessed by the gravitons. Then, one can find the typical length d [41] of the n-extra-dimensional space accessed by gravitons as

$$d = \frac{M_{\rm Pl}^{2/n}}{M_*^{1+(2/n)}} \frac{1}{\left(1 + \frac{M_{\rm Pl}^2}{M_e^2}\right)^{1/n}}, \quad (15)$$

where M_* and $M_{\rm Pl}$ are the fundamental and effective Planck scales, respectively. The extrinsic scale M_e is given by

$$\frac{1}{M_e} = \int (K^2 + h^2)\sqrt{g} d^4x, \quad (16)$$

where K^2 is the Gaussian curvature and h^2 is the mean curvature. Hence, for smooth oscillations of the embedded background, the limit imposed by Eq. (15) with the M_e scale prevents the leak of energy of the confined sources to higher-dimensional space, but it allows the graviton oscillations. This eliminates the necessity of introducing a radion field, which is commonly adopted in most popular braneworld models [32–35].

A. Background cosmology

The background cosmology is defined as usual by means of the line element of the Friedmann-Lemaître-Robertson-Walker (FLRW) four-dimensional metric as

$$ds^2 = -dt^2 + a^2(dr^2 + r^2 d\theta^2 + r^2 \sin^2\theta d\phi^2), \quad (17)$$

where the scale factor is denoted by $a \equiv a(t)$ and t is the physical time. Once the embedding is properly set, we impose that the bulk geometry is a solution of the Einstein equations given by Eq. (11). Thus, from Eqs. (8) and (9) and the confinement condition in Eq. (12), one obtains the tangent components of the nonperturbed field equations as

$$\bar{G}_{\mu\nu} - \bar{Q}_{\mu\nu} = -8\pi G \bar{T}_{\mu\nu}, \quad (18)$$

$$\bar{k}_{\mu[\nu;\rho]} = 0, \quad (19)$$

where $\bar{T}_{\mu\nu}$ is the nonperturbed energy-momentum tensor of the confined perfect fluid and G is the gravitational Newtonian constant. The background tensors $\bar{G}_{\mu\nu}$ and $\bar{Q}_{\mu\nu}$ represent the four-dimensional Einstein tensor and the *extrinsic deformation tensor*, respectively. For an arbitrary D-dimensional case, see the detailed derivation of Eqs. (18) and (19) in Ref. [42].

In addition, the nonperturbed $\bar{Q}_{\mu\nu}$ in Eq. (18) is defined as

$$\bar{Q}_{\mu\nu} = \bar{k}^\rho_\mu \bar{k}_{\rho\nu} - \bar{k}_{\mu\nu} h - \frac{1}{2}(K^2 - h^2)\bar{g}_{\mu\nu}, \quad (20)$$

where $h^2 = h \cdot h$ denotes the mean curvature with $h = \bar{g}^{\mu\nu}\bar{k}_{\mu\nu}$. The Gaussian curvature is denoted by $K^2 = \bar{k}^{\mu\nu}\bar{k}_{\mu\nu}$. A direct consequence of the previous definition in Eq. (20) is that the deformation tensor $\bar{Q}_{\mu\nu}$ is a conserved quantity, such as

$$\bar{Q}_{\mu\nu;\mu} = 0. \quad (21)$$

Solving the trace of the Codazzi equation in Eqs. (19) and (20), the following components are found [42]:

$$\bar{k}_{ij} = \frac{b}{a^2}\bar{g}_{ij}, \qquad i, j = 1, 2, 3, \quad (22)$$

$$\bar{k}_{44} = \frac{-1}{\dot{a}}\frac{d}{dt}\frac{b}{a}, \quad (23)$$

$$\bar{k}_{44} = -\frac{b}{a^2}\left(\frac{B}{H} - 1\right), \quad (24)$$

$$K^2 = \frac{b^2}{a^4}\left(\frac{B^2}{H^2} - 2\frac{B}{H} + 4\right), \qquad h = \frac{b}{a^2}\left(\frac{B}{H} + 2\right), \quad (25)$$

$$\bar{Q}_{ij} = \frac{b^2}{a^4}\left(2\frac{B}{H} - 1\right)\bar{g}_{ij}, \qquad \bar{Q}_{44} = -\frac{3b^2}{a^4}, \quad (26)$$

$$\bar{Q} = -(K^2 - h^2) = \frac{6b^2}{a^4}\frac{B}{H}, \quad (27)$$

where $\bar{Q}$ denotes the deformation scalar defined in a standard way, i.e., by the contraction $\bar{g}^{\mu\nu}\bar{Q}_{\mu\nu} = \bar{Q}$. One important definition is the evolution of the bending function $b(t) \equiv b = k_{11} = k_{22} = k_{33}$ driven by extrinsic geometry. Thus, we define $B = B(t) \equiv \frac{\dot{b}}{b} = (db/dt)/b$ as a copy of the Hubble parameter $H \equiv H(t) = \frac{\dot{a}}{a} = (da/dt)/a$. As a consequence, the $B(t)$ function uses the same units as H.

An important aspect is that in five dimensions the trace of the Codazzi equation in Eq. (19) is homogeneous, which makes the solution for the bending function $b(t)$ arbitrary. To remove such arbitrariness, we need to state the dynamics of the extrinsic curvature, since the metric and the extrinsic curvature are independent variables that must satisfy the Gauss [Eq. (8)] and Codazzi [Eq. (9)] equations. Thus, there are a total of 20 unknowns $g_{\mu\nu}$ and $k_{\mu\nu}$, against only 15 dynamical equations. This requires considering $k_{\mu\nu}$ as a source for the missing equations. A well-known theorem due to Gupta [65] states that any symmetric rank-2 tensor satisfies an Einstein-like system of equations, having the Pauli-Fierz equation as its linear approximation. In the context of strong gravity Isham *et al.* [66] proposed an f-meson spin-2 field that would act as an intermediate field between gravitation and hadron particles. In a previous publication [44], an Einstein-like dynamical equation for the extrinsic curvature was adapted from the original equation of Gupta. Using Gupta's theorem, as shown in [44,49], one simply obtains

$$b(t) = b_0 a(t)^{\beta_0}, \tag{28}$$

where the term b_0 is the current value of the bending function and β_0 is an integration constant. As we are going to show, it is associated with the fluid parameter w. Accordingly, the Friedmann equation in terms of redshift can be written in the form

$$\left(\frac{H}{H_0}\right)^2 = \Omega_{m(0)}(1+z)^3 + \Omega_{\mathrm{rad}(0)}(1+z)^4 + \Omega_{\mathrm{ext}(0)}(1+z)^{4-2\beta_0}, \tag{29}$$

where $\Omega_{m(0)}$ denotes the current cosmological parameter for the matter density content. The radiation content is denoted by $\Omega_{\mathrm{rad}(0)} = \Omega_{m0} z_{\mathrm{eq}}$, wherein the equivalence number for the expansion factor a_{eq} is

$$a_{\mathrm{eq}} = \frac{1}{1+z_{\mathrm{eq}}} = \frac{1}{(1 + 2.5\times 10^4 \Omega_{m(0)} h^2 (T_{\mathrm{CMB}}/2.7)^{-4})}, \tag{30}$$

where z_{eq} is the equivalence redshift. The adopted value for the CMB temperature is $T_{\mathrm{CMB}} = 2.7255$ K and the Hubble factor $h = 0.67$ [10]. The term $\Omega_{\mathrm{ext}(0)}$ stands for the density parameter associated with the extrinsic curvature. For a flat universe, $\Omega_{\mathrm{ext}(0)} = 1 - \Omega_{m(0)} - \Omega_{\mathrm{rad}(0)}$. Moreover, the current extrinsic cosmological parameter $\Omega_{\mathrm{ext}(0)}$ is defined as

$$\Omega_{\mathrm{ext}(0)} = \frac{8\pi G}{3H_0^2}\rho_{\mathrm{ext}(0)} \equiv \frac{b_0^2}{H_0^2 a_0^{\beta_0}}, \tag{31}$$

where a_0 sets the current value of the scale factor and $\rho_{\mathrm{ext}(0)} \equiv \frac{3}{8\pi G} b_0^2$ denotes the current extrinsic density.

B. Perturbations in conformal Newtonian gauge

The perturbed equations are necessary for the right estimation of cosmological parameters. In this framework, the relevant modifications of field equations under cosmological perturbations are applied to the lhs of Eq. (18) with the presence of $\bar{Q}_{\mu\nu}$ and the $\bar{G}_{\mu\nu}$ and $\bar{T}_{\mu\nu}$ tensors, which are treated in a very standard fashion, as shown in Ref. [44]. Thus, for a fluid with pressure P and density $\bar{\rho}$, the perturbed components of the stress-tensor energy $\delta T_{\mu\nu}$ are given as

$$\delta T^i_j = \delta p \delta^i_j + \Sigma^i_j, \tag{32}$$

$$\delta T^4_4 = -\delta\rho, \tag{33}$$

$$\delta T^4_i = \frac{1}{a}(\bar{\rho} + P)\delta u_{\parallel i}, \tag{34}$$

where $\delta u_{\parallel i}$ is the tangent velocity potential of the fluid. The anisotropic stress tensor is defined as $\Sigma^i_j = T^i_j - \delta^i_j T^k_k/3$. Moreover, the only relevant field equations that propagate cosmological perturbations are given by

$$\delta G^\mu_\nu - \delta Q^\mu_\nu = -8\pi G \delta T^\mu_\nu. \tag{35}$$

In addition, we have to determine the perturbed extrinsic terms given by $\delta Q_{\mu\nu}$. Using the Nash relation of Eqs. (5) and (7), one obtains

$$\delta k_{\mu\nu} = \bar{g}^{\sigma\rho} \bar{k}_{\mu\sigma} \delta g_{\nu\rho}. \tag{36}$$

This is a pivot result since it shows how the effects of the extrinsic quantities are projected onto the embedded four dimensional space-time and how the Nash flow of Eq. (5) is connected to cosmological perturbations. Hence, the perturbations of the deformation tensor $\bar{Q}_{\mu\nu}$ are given in the form

$$\delta Q_{\mu\nu} = -\frac{3}{2}(K^2 - h^2)\delta g_{\mu\nu}. \tag{37}$$

Alternatively, we construct a relation of the equations in a fluid approach by writing the gravitensor equation [Eq. (18)] in a general form as

$$G_{\mu\nu} = -8\pi G T^{\mathrm{total}}_{\mu\nu}, \tag{38}$$

where the tensors are written using the composition of their background and perturbed components. The related Einstein tensor is written as $G_{\mu\nu} = \bar{G}_{\mu\nu} + \delta G_{\mu\nu}$, $T^{\mathrm{total}}_{\mu\nu} = T_{\mu\nu} + T^{\mathrm{ex}}_{\mu\nu}$, where $T_{\mu\nu} = \bar{T}_{\mu\nu} + \delta T_{\mu\nu}$ and $T^{\mathrm{ex}}_{\mu\nu} = \bar{T}^{\mathrm{ex}}_{\mu\nu} + \delta T^{\mathrm{ex}}_{\mu\nu}$.

In the conformal Newtonian gauge, the FLRW metric is given by

$$ds^2 = a^2[-(1+2\Psi)d\tau^2 + (1-2\Phi)dx^i dx_i], \quad (39)$$

where $\Psi = \Psi(\vec{x}, \tau)$ and $\Phi = \Phi(\vec{x}, \tau)$ denote the Newtonian potential and the Newtonian curvature in conformal time τ that is defined as $d\tau = dt/a(t)$. Hence, we determine the confined matter fields represented by the nonperturbed stress-energy tensor $\bar{T}_{\mu\nu}$ in a comoving fluid such as

$$\bar{T}_{\mu\nu} = (\bar{\rho} + P)U_\mu U_\nu + P\bar{g}_{\mu\nu}; \qquad U_\mu = \delta^4_\mu, \quad (40)$$

where U_μ denotes the comoving velocity. The related conservation equation is given by

$$\bar{\rho} + 3H(\bar{\rho} + P) = 0. \quad (41)$$

From the perturbed conservation equation $\delta T_{\mu\nu;\nu} = 0$, the evolution equations can be obtained for the "contrast" matter density δ_m and fluid velocity θ, such as

$$\dot{\delta_m} = -(1+w)(\theta - 3\dot{\Phi}) - 3H(c_s^2 - w)\delta_m, \quad (42)$$

$$\dot{\theta} = -H(1-3w)\theta - \frac{\dot{w}}{1+w}\theta + \frac{c_s^2}{1+w}k^2\delta_m - k^2\sigma + k^2\Psi, \quad (43)$$

where $\theta = ik^j u_j$, w is the fluid parameter $w = \frac{P}{\bar{\rho}}$, c_s^2 is the sound velocity defined as $c_s^2 = \frac{\delta P}{\delta\rho}$, and σ is the anisotropic stress. The dot symbol denotes the ordinary derivative with respect to conformal time τ.

To avoid divergences when the equation of state crosses $w = -1$, eventually, the scalar velocity $V = (1+w)\theta$ should be defined [67,68]. Hence, we have the equations

$$\delta_m' = 3(1+w)\Phi' - \frac{V}{a^2 H} - \frac{3}{a}\left(\frac{\delta P}{\bar{\rho}} - w\delta_m\right), \quad (44)$$

$$V' = -(1-3w)\frac{V}{a} + \frac{k^2}{a^2 H}\frac{\delta P}{\bar{\rho}} + (1+w)\frac{k^2}{a^2 H}\Psi - \frac{k^2}{a^2 H}(1+w)\sigma, \quad (45)$$

where the prime symbol $'$ denotes the ordinary derivative with respect to the scale factor as $' = \frac{d}{da}$.

For the induced extrinsic part, the term $8\pi G\bar{T}^{\rm ext}_{\mu\nu} \doteq \bar{Q}_{\mu\nu}$ is written as copy of a perfect fluid as

$$-8\pi G\bar{T}^{\rm ext}_{\mu\nu} = (\bar{p}_{\rm ext} + \bar{\rho}_{\rm ext})U_\mu U_\nu + \bar{p}_{\rm ext}\bar{g}_{\mu\nu}, \qquad U_\mu = \delta^4_\mu, \quad (46)$$

where U_μ is the comoving four-velocity. Since $T_{\mu\nu;\nu} = 0$ and $T^{\rm ext}_{\mu\nu;\nu} = 0$ [as a consequence of Eq. (21)], $T^{\rm total}_{\mu\nu}$ is conserved. Hence, the conservation equation for extrinsic quantities is given by

$$\frac{d\bar{\rho}_{\rm ext}}{dt} + 3H(\bar{\rho}_{\rm ext} + \bar{p}_{\rm ext}) = 0, \quad (47)$$

where $\bar{\rho}_{\rm ext}$ and $\bar{p}_{\rm ext}$ denote the nonperturbed extrinsic density and extrinsic pressure, respectively. The time-time and space-time components of $T^{\rm ext}_{\mu\nu}$ can be set as

$$-8\pi G T^{\rm ext}_{44} = \bar{T}^{\rm ext}_{44} + \delta T^{\rm ext}_{44} = \bar{Q}_{44} + \delta Q_{44}, \quad (48)$$

$$-8\pi G T^{\rm ext}_{i4} = \bar{T}^{\rm ext}_{i4} + \delta T^{\rm ext}_{i4} = \bar{Q}_{i4} + \delta Q_{i4} = 0. \quad (49)$$

The modified Friedman equation is written as

$$H^2 = \frac{8}{3}\pi G(\bar{\rho}_m + \bar{\rho}_{\rm rad} + \bar{\rho}_{\rm ext}), \quad (50)$$

where $\bar{\rho}_{\rm ext}(a)$ is given by

$$\bar{\rho}_{\rm ext}(a) = \bar{\rho}_{\rm ext}(0)a^{2\beta_0 - 4}, \quad (51)$$

with $\bar{\rho}_{\rm ext}(0) = \frac{3}{8\pi G}b_0^2$. Once $\bar{\rho}_{\rm ext}(a)$ is already determined, the "extrinsic" pressure can be calculated using Eqs. (47) and (51) to obtain

$$\bar{p}_{\rm ext}(a) = \frac{1}{3}(1 - 2\beta_0)\bar{\rho}_{\rm ex}(0)a^{2\beta_0 - 4}. \quad (52)$$

For positive values of β_0, the null energy conditions (NECs) is satisfied. If $\beta_0 = 2$, the extra term in the modified Friedmann equation in Eq. (29) mimics a cosmological constant. If $\beta_0 > 2$, the effective behavior becomes phantom-like. However, the condition $\beta_0 > 1$ is required if the Universe must accelerate (apart from being consistent with the NECs). Thus, we define an effective equation of state with an "extrinsic fluid" parameter $w_{\rm ext}$ using the definition $w_{\rm ext} = \frac{\bar{p}_{\rm ext}}{\bar{\rho}_{\rm ext}}$ to obtain

$$w_{\rm ext} = -1 + \frac{1}{3}(4 - 2\beta_0). \quad (53)$$

Thus, when

$$\beta_0 = 2 - \frac{3}{2}(1+w), \quad (54)$$

one has the fluid correspondence $w_{\rm ext} = w$. This allows us to express all of the relevant quantities in a fluid approach. For instance, the dimensionless Hubble parameter $E(z) = \frac{H(z)}{H_0}$ is written as

$$E^2(z) = \Omega_{m(0)}(1+z)^3 + \Omega_{\rm rad(0)}(1+z)^4 + \Omega_{\rm ext(0)}(1+z)^{3(1+w)}. \quad (55)$$

For reference, we name this model the β model.

From Eq. (37), we calculate the set of nonzero components of $\delta Q_{\mu\nu}$ using the background relations in Eqs. (22) and (25)–(27). Then, one obtains

$$\delta Q^4_4 = \gamma_0 a^{-(1+3w)} \Psi \delta^4_4, \tag{56}$$

$$\delta Q^i_j = \gamma_0 a^{-(1+3w)} \Phi \delta^i_j, \tag{57}$$

$$\delta Q^i_i = 3\gamma_0 a^{-3(1+w)} \Phi, \tag{58}$$

$$\delta Q = \gamma_0 (3\Psi - \Phi) a^{-3(1+w)}. \tag{59}$$

For the sake of notation and using Eq. (31) in the previous set of equations, γ_0 denotes

$$\gamma_0 = 18 b_0^2 \beta_0 = 9 H_0^2 \Omega_{\mathrm{ext}(0)} \gamma_s, \tag{60}$$

where β_0 was simplified by introducing the γ_s parameter, which is regarded as a relic from extrinsic geometry to maintain the characteristic of the parameter γ_0. Moreover, it makes γ_0 in Eq. (60) independent of the nature of the fluid characterized by the w parameter, as expected. This is also necessary to maintain the GR correspondence that is reached when the extrinsic curvature vanishes, i.e., $\gamma_s \to 0$.

From Eq. (38) one writes the gauge-invariant perturbed field equations in the Fourier k-space wave modes as

$$k^2 \Phi_k + 3\mathcal{H}(\Phi'_k + \Psi_k \mathcal{H}) = -4\pi G a^2 \delta\rho_k + \chi(a) \Psi_k, \tag{61}$$

$$\Phi'_k + \mathcal{H}\Psi_k = -4\pi G a^2 (\bar{\rho} + P) \frac{\theta}{k^2}, \tag{62}$$

$$\mathcal{D}_k + \frac{k^2}{3}(\Phi_k - \Psi_k) = -\frac{4}{3}\pi G a^2 \delta\bar{P} - \frac{1}{2} a^2 \delta Q^i_i, \tag{63}$$

$$k^2 (\Phi_k - \Psi_k) = 12\pi G a^2 (\bar{\rho} + P)\sigma, \tag{64}$$

where $\theta = i k^j \delta u_{\|j}$ denotes the divergence of the fluid velocity in k-space and $\mathcal{D}_k$ denotes $\mathcal{D}_k = \Phi''_k + \mathcal{H}(2\Phi_k + \Psi_k)' + (\mathcal{H}^2 + 2\mathcal{H}')\Psi_k$. The function $\chi(a)$ is expressed in terms of the cosmological parameters and reads

$$\chi(a) = \frac{9}{2} \gamma_s \frac{H_0^2}{\Omega_{\mathrm{rad}}(a)} \Omega_{\mathrm{rad}}(0) \Omega_{\mathrm{ext}}(a). \tag{65}$$

III. EMBEDDING AS A MODIFIED GRAVITY MODEL

After some algebra, the set of perturbed equations in Eqs. (61)–(64) is simplified to the following set of equations:

$$k^2 \Psi_k = -4\pi G a^2 \mu(a,k) \rho\Delta, \tag{66}$$

$$k^2 (\Phi_k + \Psi_k) = -8\pi G a^2 \Sigma(a,k) \rho\Delta, \tag{67}$$

where $\rho\Delta = \bar{\rho}\delta + 3\frac{\mathcal{H}}{k}(\bar{\rho} + P)\theta$. The set of equations (66) and (67) is valid for all times. When anisotropic stress is neglected, $\mu(a,k)$ and $\Sigma(a,k)$ can be written as

$$\mu(a,k) = \frac{1}{1 - \frac{\chi(a)}{k^2}}, \tag{68}$$

$$\Sigma(a,k) = \frac{1}{2}\left[1 + \mu(a,k)\left(1 + \frac{\chi(a)}{k^2}\right)\right]. \tag{69}$$

Using the definition of the slip function $\gamma(a,k) = \frac{\Phi}{\Psi}$, from Eqs. (68) and (69), one easily obtains

$$\Sigma(a,k) = \frac{1}{2}\mu(a,k)(1 + \gamma(a,k)). \tag{70}$$

When the extrinsic term $\gamma_s \to 0$ in order to recover general relativity (GR) correspondence, one obtains the standard GR limit as $\Sigma(a,k) = \mu(a,k)$ and $\gamma(a,k) = 1$. Thus, the set of basic equations is complete with the matter perturbation equations in Eqs. (44) and (45) and the evolution equation of Φ. To obey Solar constraints, γ_s in $\mu(a,k)$ must comply with the condition

$$\gamma_s < \frac{0.222 k_p^2}{H_0^2 \Omega_{\mathrm{ext}(0)}}, \tag{71}$$

at the pivot scale wave number k_p. For instance, adopting baseline mean values of 68% intervals of the base ΛCDM model from *Planck* TT, TE, EE + lowE + lensing [10], we obtain $\gamma_s < 3.219 \times 10^{-8}$, which means that the deviation of MG should be pronounced below that cutoff.

IV. EXTRINSIC CURVATURE AS AN EFFECTIVE INFLATON FIELD

In previous publications [44,48,49], we explored some of the consequences of the Nash embedding in the context of the dark energy problem. The appearance of the extrinsic energy density $\bar{\rho}_{\mathrm{ext}}$ drives the Universe to the late accelerated expansion and the Friedmann equation is written in a shorter form as

$$H^2 = \frac{\kappa^2}{3}(\bar{\rho} + \bar{\rho}_{\mathrm{ext}}), \tag{72}$$

with $\kappa = 8\pi G$ and $\bar{\rho} = \bar{\rho}_m + \bar{\rho}_{\mathrm{rad}}$. In terms of inflationary cosmology, such an energy density $\bar{\rho}_{\mathrm{ext}}$ should provide a response in the form of a scalar field potential $V(\phi)$ generated by a spatially homogeneous "extrinsic" scalar field ϕ [50]. Thus, one defines a Lagrangian $\mathcal{L}_\phi$ as

$$\mathcal{L}_\phi = \frac{1}{2}\dot{\phi}^2 - V(\phi), \tag{73}$$

where the time derivative is represented by the dot symbol. Immediately, one writes the related energy-momentum tensor as

$$T^\phi_{\mu\nu} = \partial_\mu\phi\partial_\nu\phi + g_{\mu\nu}\left(\frac{1}{2}\dot{\phi}^2 - V(\phi)\right). \tag{74}$$

From the conservation of Eq. (74), the inflation dynamics is coupled to the background evolution and we obtain the relations

$$\bar{\rho}_{\rm ext} = \frac{\dot{\phi}^2}{2} + V(\phi), \tag{75}$$

$$\bar{p}_{\rm ext} = \frac{\dot{\phi}^2}{2} - V(\phi), \tag{76}$$

where $\bar{\rho}_{\rm ext}$ and $\bar{p}_{\rm ext}$ denote the energy density and pressure generated by extrinsic curvature as a function of the extrinsic scalar field ϕ, respectively.

As shown in Ref. [50], using Eqs. (51)–(53), (75), and (76), by direct integration, one obtains the potential $\phi(a)$ as

$$\phi(a) = \sqrt{|3(1+w)|}M_{\rm pl}\ \ln\, a. \tag{77}$$

Hereafter, we denote the reduced Planck mass as $M_{\rm pl} = \frac{1}{\sqrt{8\pi G}} = c = 1$. The potential $V(\phi)$ is also obtained straightforwardly as

$$V(\phi) = V_0 e^{-\alpha_0\phi}, \tag{78}$$

where $\alpha_0 = \sqrt{|3(1+w)|}$. This kind of exponential model is well known in the literature and is commonly referred to as *power-law inflation* (PLI) [69–72]. Such a potential was also studied in the context of M-theory [73] and Randall-Sundrum II scenarios [74]. Due to the strong constraints imposed by *Planck* data [75] on PLI, we follow the generalization proposed in Refs. [76,77] called β-exponential inflation. In Ref. [76], the authors introduced a class of potentials in the form

$$\begin{aligned} V(\phi) &= V_0 \exp_{1-\beta}(-\lambda\phi/M_{\rm pl}) \\ &= V_0[1+\beta(-\lambda\phi/M_{\rm pl})]^{1/\beta}. \end{aligned} \tag{79}$$

In general, the function $\exp_{1-\beta}(f) = [1+\beta f]^{1/\beta}$ may be $1+\beta f > 0$ or $\exp_{1-\beta}(f) = 0$. Then, Eq. (79) should satisfy the identities $\exp_{1-\beta}(\ln_{1-\beta}(f)) = f$ and $\ln_{1-\beta}(f) + \ln_{1-\beta}(g) = \ln_{1-\beta}(fg) - \beta[\ln_{1-\beta}(f)\ln_{1-\beta}(g)]$ for any $g < 0$. The term $\ln_{1-\beta}(f) = (f^\beta - 1)/\beta$ is referred to as the generalized logarithm function. For our purposes, Eq. (78) can be generalized to Eq. (79) in the form

$$V(\phi) = V_0[1-\beta\alpha_0\phi]^{1/\beta}. \tag{80}$$

Assuming that the field starts rolling in a local minimum as $\frac{\partial^2 V(\phi)}{\partial^2\phi} = 0$ for any $\beta \neq 1$, starting at $\phi = \phi_{\rm min} = 1$, one obtains the condition $\beta = \frac{1}{\alpha_0} > 0$. Thus, we can write Eq. (80) as

$$V(\phi) = V_0[1-\phi]^{\alpha_0}. \tag{81}$$

Then, one defines the pair of slow-roll parameters

$$\varepsilon = \frac{1}{2\kappa}\left(\frac{V_{,\phi}}{V}\right)^2, \tag{82}$$

$$\eta = \frac{1}{\kappa}\frac{V_{,\phi\phi}}{V}. \tag{83}$$

In order to submit the model to the scrutiny of observational data, they are expressed as

$$\eta_s = 1 - 6\varepsilon + 2\eta, \tag{84}$$

$$r = 16\varepsilon, \tag{85}$$

where η_s is the spectral tilt and r is the tensor-to-scalar ratio. The relation between the parameters is given by

$$\eta_s = 1 - \frac{\alpha_0(\alpha_0+2)}{(1-\phi_\star)^2}, \tag{86}$$

$$r = \frac{8\alpha_0^2}{(1-\phi_\star)^2}, \tag{87}$$

where $\phi_\star$ is the field before the end of inflation given by

$$\phi_\star = 1 - \alpha_0\sqrt{0.5 + \frac{2}{\alpha_0}N}. \tag{88}$$

The quantity N denotes the number of e-folds before the end of inflation and is defined as

$$N = \int_{\phi_{\rm end}}^{\phi_\star} \frac{d\phi}{2\sqrt{\varepsilon}} = \frac{\phi_\star^2}{2\alpha_0} - \frac{\phi_\star}{\alpha_0} + \frac{1}{2\alpha_0} - \frac{\alpha_0}{4}. \tag{89}$$

At the end of inflation, the field $\phi_{\rm end}$ is calculated from the condition $\varepsilon(\phi_{\rm end}) \sim 1$, and one finds

$$\phi_{\rm end} = 1 - \frac{\alpha_0\sqrt{2}}{2}. \tag{90}$$

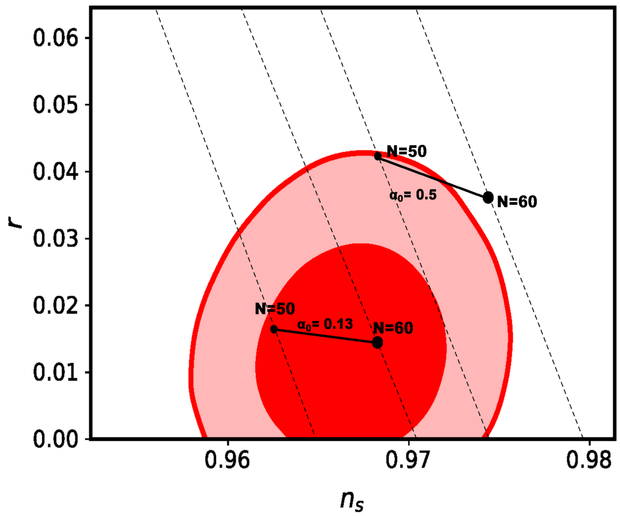

FIG. 1. $\eta_s - r$ plane for the range of values of the parameter α_0 in Eq. (78), for the number of e-folds $N = 50$ and $N = 60$. The contours correspond to joint fitting *Planck* + BK18 + LSS (68% and 95% CL) [55] at the pivot scale $k_p = 0.05\ \mathrm{Mpc}^{-1}$.

The slow-roll parameters as functions of ϕ are given by

$$\varepsilon(\phi) = \frac{\alpha_0^2}{2(1-\phi)^2}, \tag{91}$$

$$\eta(\phi) = \frac{\alpha_0(\alpha_0 - 2)}{2(1-\phi_\star)^2}. \tag{92}$$

Figure 1 shows the $\eta_s - r$ plane for selected values of the parameter α_0 in Eq. (78) for the number of e-folds $N = 50$ and $N = 60$. The 68% and 95% CL contours correspond to joint fitting *Planck* (2018) + BK18 + LSS extracted from publicly available CosmoMC chains [55]. Examining the behavior of the α_0 parameter, we end up concluding that higher values of α_0 for the prediction of r are in agreement with observations but compromise the prediction of the spectral index η_s. In contrast, lower values of α_0 (it is worth noting that $\alpha_0 = 0$ mimics ΛCDM) are consistent with *Planck* data at the 1σ CL for the tensor-to-scalar ratio r. In this case, $\alpha_0 = 0.13$ and $\alpha_0 = 0.5$ suggest that $w = -0.9944$ and $w = -0.9167$, respectively. On the other hand, when considering the combinations with HiLLiPoP and LoLLiPoP likelihoods [75] with BICEP2/Keck 2015 data [78] as hlpTT + lowT + lowlEB and hlpTT + lowT+ lowlEB + BK15, $\alpha_0 = 0.5$ is compatible at the 1σ and 2σ CL.

V. DATA AND METHODOLOGY

To delineate constraints on the free parameter of our model, we examine several data sets individually as well as in various combinations. Specifically, we consider the following:

(1) Utilizing the latest NPIPE *Planck* DR4 likelihoods [53,54] of the *Planck* 2018 legacy data release, our analysis incorporates CMB measurements. These include the high-ℓ Plik TT likelihood spanning the multipole range $30 \le \ell \le 2508$, as well as TE and EE measurements within the multipole range $30 \le \ell \le 1996$. Additionally, we incorporate low-ℓTT-only ($2 \le \ell \le 29$) and EE-only ($2 \le \ell \le 29$) likelihoods. Furthermore, our data set encompasses CMB NPIPE *Planck* lensing power spectrum measurements, collectively referred to as the *Planck* data set.

(2) The B-mode polarization data from the BICEP2/Keck Collaboration [55]. We refer to this data set as `BK18`.

(3) We refer to this data set as `LSS`. We consider the 6dF Galaxy Survey [56], the SDSS DR7 MGS [57] and clustering measurements of eBOSS associated with the SDSS's Sixteenth Data Release [58]. This collection encompasses data from luminous red galaxies, emission line galaxies, quasars, the Lyman-alpha forest autocorrelation (*lyauto*), and the Lyman-alpha forest x quasar cross-correlation (*lyxqso*). Table I details the diverse baryon acoustic oscillation (BAO) components considered in this work.

(a) The Hubble distance at redshift z:

$$D_H(z) = \frac{c}{H(z)}, \tag{93}$$

where $H(z)$ is the Hubble parameter.

TABLE I. Data sets from SDSS employed in our analysis.

Data set ID	Description	Reference
sixdf_2011_bao	6dF Galaxy Survey	[56]
sdss_dr7_mgs	SDSS DR7 MGS	[57]
sdss_dr16_baoplus_lrg	BOSS DR16—Luminous red galaxies	[58]
sdss_dr16_baoplus_elg	BOSS DR16—Emission line galaxies	[79]
sdss_dr16_baoplus_qso	BOSS DR16—Quasars	[79]
sdss_dr16_baoplus_lyauto	BOSS DR16—Lyman-alpha forest autocorrelation	[79]
sdss_dr16_baoplus_lyxqso	BOSS DR16—Lyman-alpha forest x quasar cross-correlation	[79]

TABLE II. Summary of 68% and 95% CL limits for the parameters of interest obtained from *Planck* + BK18 and *Planck* + BK18 + LSS joint data at the pivot scale $k_p = 0.05\ \mathrm{Mpc}^{-1}$.

	Planck + BK18		*Planck* + BK18 + LSS	
Parameter	68% CL	95% CL	68% CL	95% CL
n_s	0.9646 ± 0.0031	$0.9646^{+0.0057}_{-0.0060}$	0.9648 ± 0.0030	$0.9648^{+0.0056}_{-0.0060}$
r	$0.0142^{+0.0049}_{-0.012}$	< 0.0307	$0.0139^{+0.0044}_{-0.013}$	< 0.0303
H_0	66.981 ± 0.078	$66.98^{+0.15}_{-0.15}$	67.001 ± 0.078	$67.00^{+0.15}_{-0.15}$
Ω_m	0.31794 ± 0.00074	$0.3179^{+0.0014}_{-0.0015}$	0.31776 ± 0.00074	$0.3178^{+0.0014}_{-0.0014}$
$\mu - 1$	$-0.01^{+0.17}_{-0.21}$	$-0.01^{+0.40}_{-0.34}$	0.02 ± 0.15	$0.02^{+0.30}_{-0.28}$
$\Sigma - 1$	$-0.053^{+0.051}_{-0.042}$	$-0.053^{+0.093}_{-0.098}$	$-0.049^{+0.048}_{-0.042}$	$-0.049^{+0.083}_{-0.091}$
$10^8 \gamma_s$	$-0.3^{+3.1}_{-3.8}$	$-0.3^{+7.2}_{-6.2}$	0.3 ± 2.7	$0.3^{+5.4}_{-5.0}$

(b) The comoving angular diameter distance, $D_M(z)$, which also only depends on the expansion history:

$$D_M(z) = \frac{c}{H_0} \int_0^z dz' \frac{H_0}{H(z')}. \tag{94}$$

(c) The spherically averaged BAO distance:

$$D_V(z) = r_d [z D_M^2(z) D_H(z)]^{1/3}, \tag{95}$$

where r_d is the BAO scale, which we treat as a derived parameter in our analyses.

For the growth measurements, the growth function f can be expressed as a differential in the amplitude of linear matter fluctuations on a comoving scale of 8 h^{-1} Mpc, $\sigma_8(z)$, in the form

$$f(z) = \frac{\partial \ln \sigma_8}{\partial \ln a}. \tag{96}$$

The RSD measurements provide constraints on the quantity $f(z)\sigma_8(z)$. $\sigma_8(z)$ depends on the matter power spectrum, $P(k, z)$, which is calculated by default in the Boltzmann code. Both $f(z)$ and $\sigma_8(z)$ are sensitive to variations in the effective gravitational coupling and the light deflection parameter, which play a crucial role in Poisson and lensing equations in MG models.

The joint likelihood analysis is conducted using MGCAMB-II [59] through the Cobaya [60] sampler, employing the $\mu - \Sigma$ parametrization defined as follows:

$$\mu(a, k) = 1 + \mu_0 \frac{\Omega_{\mathrm{DE}}}{\Omega_{DE(0)}}, \tag{97}$$

$$\Sigma(a, k) = 1 + \Sigma_0 \frac{\Omega_{\mathrm{DE}}}{\Omega_{DE(0)}}. \tag{98}$$

Here, $\Omega_{\mathrm{DE}}(a)$ is denoted as the extrinsic contribution $\Omega_{\mathrm{ext}}(a)$, which means that $\Omega_{DE(0)} = \Omega_{\mathrm{ext}}(0) = 1 - \Omega_{m(0)}$. The forms of Eqs. (97) and (98) in this parametrization are obtained from expanding the function $\chi(a) \ll 1$ in the denominator of Eq. (68). We assume a pivot scale fixed at $a_p = 10^{-4}$ and $k_p = 0.05\ \mathrm{Mpc}^{-1}$. It is worth noting that the anisotropic stress is not considered in our analysis.

The priors on the baseline parameters utilized in our analysis are detailed in Table II. In all runs, we ensure a Gelman-Rubin convergence criterion of $R - 1 < 0.03$. In the subsequent section, we will unveil the outcomes of our Bayesian analysis and delve into their implications.

VI. RESULTS

We commence our analysis by scrutinizing the constraints derived exclusively from the joint analysis of the *Planck* and BK18 data sets. The primary statistical findings concerning the cosmological parameters of interest are summarized in Table III.

We analyze the results by examining the parameters that indicate deviations from the standard ΛCDM cosmology. Figure 2 illustrates the parameter space for γ_s, μ, and Σ.

Figure 3 shows the $n_s - r$ plane. We note that the tensor-to-scalar ratio r effects arise from MG scenario outlined in this study. In canonical parametric $P(k)$ inflation and ΛCDM dynamics, $r < 0.036$ at 95% CL [29] is found, whereas for the present modified scenario, we find a $r < 0.0307$ at 95% CL with *Planck* + BK18 data. This represents a variation of $\Delta r = 0.03$ as compared with standard model, suggesting the signature of an MG model.

TABLE III. The cosmological parameters along with their respective priors employed in the parameter estimation analysis.

Parameter	Prior
$\Omega_b h^2$	$\mathcal{U}[0.017, 0.027]$
$\Omega_c h^2$	$\mathcal{U}[0.09, 0.15]$
θ_{MC}	$\mathcal{U}[0.0103, 0.0105]$
τ_{reio}	$\mathcal{N}[0.065, 0.0015]$
$\log(10^{10} A_s)$	$\mathcal{U}[2.6, 3.5]$
n_s	$\mathcal{U}[0.9, 1.1]$
$10^8\ \gamma_s$	$\mathcal{U}[-1, 1]$

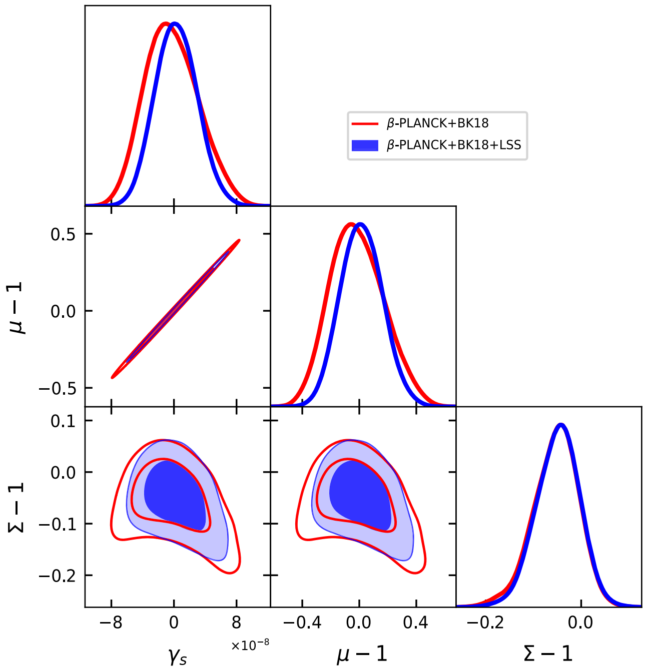

FIG. 2. Triangle plot contours with MG parameters $\mu - \Sigma$ and the γ_s parameter of the β model for the combined analyses of *Planck* + BK18 (red line) and *Planck* + BK18 + LSS (blue line).

At the pivot scale $k_p = 0.05\ \mathrm{Mpc}^{-1}$, our result is compatible with the upper bounds predicted by current *Planck* data [75] with $r < 0.032$ at 95% CL from E- and B-mode spectra BK18 [55] and LSS data [79]. In addition, our upper constraint on r with $r < 0.0307$ at 95% CL is also tighter than the standard joint data *Planck* + BK18 with $r < 0.036$ and NPIPE (PR4) with $r < 0.056$ at 95% CL. Our results indicate a lower value for r as compared with the observations from the PR4 *BB* spectrum for multipoles between $l = 2$ and $l = 150$ with $r = 0.033 \pm 0.069$ [75]. In contrast with the frequentist profile likelihood method [30] with an upper limit of $r < 0.037$ at 95% CL, we also obtain a tighter constraint on r for the same combination of *Planck*, BK18, and LSS with $r < 0.0303$ at 95% CL. In this context, our inflationary model partially constrains data better than the ΛCDM model does.

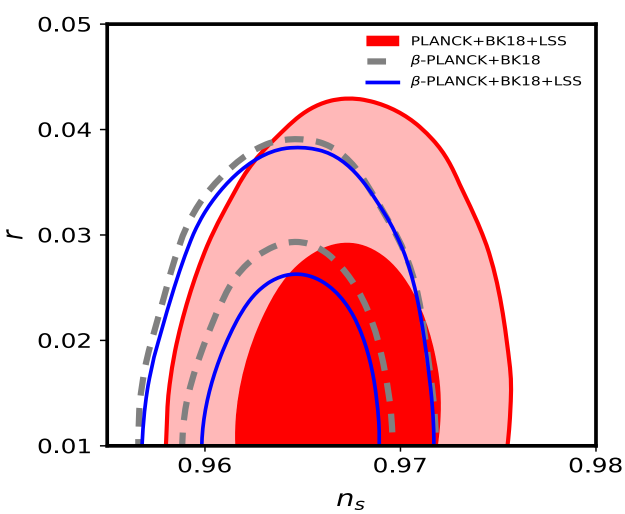

FIG. 3. Contours in the $n_s - r$ plane, delineating the 68% and 95% CL, represent the combined analyses of *Planck* + BK18 (grey dashed line contour) and *Planck* + BK18 + LSS (blue line contour) using the β model. The red contour illustrates the joint fitting of *Planck* + BK18 + LSS extracted from publicly available CosmoMC chains [55]. For interpretation of the references to color in this figure legend, the reader is referred to the web version of this article.

Considering the scalar spectral index n_s, we obtain a value of $n_s = 0.9641 \pm 0.0031$ with *Planck* + BK18 + LSS data at 68% CL which is close to base ΛCDM *Planck* TT, TE, EE + lowE + lensing with $n_s = 0.9649 \pm 0.0042$ at 68% CL and $n_s = 0.9665 \pm 0.0038$ at 68% CL when considering *Planck* TT, TE, EE + lowE + lensing + LSS. On the other hand, the small differences between the n_s value seem to affect the value of H_0, which is roughly 0.5% lower than the *Planck*-ΛCDM case. From the *Planck* + BK18 + LSS data set, in the analysis of slow-roll parameters, the model prefers the case where $\alpha_0 = 0.13$ gives $w = -0.9944$, as shown in Fig. 1 for the number of e-folds $N = 50$ and $N = 60$. Most importantly, the model does not require a larger number of e-folds to provide a tighter constraint on r. We also verified that the inclusion of LSS data does not significantly change the value of n_s but influences the H_0 values, which may be improved with upcoming new constraints on the reionization optical depth whose uncertainties may provoke a large impact on fundamental cosmological parameters such as n_s [80].

VII. FINAL REMARKS

In this paper, we have derived the gravitational equations within four dimensions by inducing them from a five-dimensional bulk, employing the Nash embeddings framework and incorporating them into a well-established $\mu - \Sigma$ representation. From the analysis of the slow-roll conditions, we have obtained a PLI model that was generalized to the β-exponential inflation [76,77]. We obtained $w = -0.9944$ for the number of e-folds in the range $N = 50$ and $N = 60$. Interestingly, this model also sits within the previous reasonable expected number of e-folds compatible with the tighter restriction on r, which is important to maintain the window of solving the horizon problem. This enabled us to assess and investigate the impact of the model on linear perturbations in the CMB data. Apart from the values of the tensor-to-ratio parameter, our primary analyses revealed similar predictions to those of the ΛCDM model. Additionally, we quantified the model's predictions concerning inflationary dynamics. By utilizing data from CMB-PR4, BICEP/Keck Array 2018, and certain LSS measurements, we established a tighter upper limit of $r < 0.0303$ at 95% CL. As compared with the ΛCDM model, such apparent improvement of the tensor-to-ratio parameter and a similar but lower value of the scalar spectral index n_s may suggest the glimpse of an MG signature, which may be improved in future experiments.

ACKNOWLEDGMENTS

A. J. S. C. thanks the financial support from the Conselho Nacional de Desenvolvimento Científico e Tecnológico (CNPq, National Council for Scientific and Technological Development) for partial financial support under the Project No. 305881/2022-1, and the Fundação da Universidade Federal do Paraná (FUNPAR, Paraná Federal University Foundation) by public notice 04/2023-Pesquisa/PRPPG/UFPR- for partial financial support under process nº 23075.019406/2023-92. R. C. N. thanks the financial support from CNPq under the Project No. 304306/2022-3, and the Fundação de Amparo à pesquisa do Estado do RS (FAPERGS, Research Support Foundation of the State of RS) for partial financial support under the Project No. 23/2551-0000848-3.

[1] A. H. Guth, Inflationary universe: A possible solution to the horizon and flatness problems, Phys. Rev. D **23**, 347 (1981).

[2] A. A. Starobinsky, Spectrum of relict gravitational radiation and the early state of the universe, JETP Lett. **30**, 682 (1979), http://jetpletters.ru/ps/1370/article_20738.shtml.

[3] V. F. Mukhanov and G. V. Chibisov, Quantum fluctuations and a nonsingular universe, JETP Lett. **33**, 532 (1981), http://jetpletters.ru/ps/1510/article_23079.shtml.

[4] A. D. Linde, Chaotic inflation, Phys. Lett. **129B**, 177 (1983).

[5] S. Hawking, The development of irregularities in a single bubble inflationary universe, Phys. Lett. **115B**, 295 (1982).

[6] S. Hawking and I. Moss, Fluctuations in the inflationary universe, Nucl. Phys. **B224**, 180 (1983).

[7] A. Starobinsky, Dynamics of phase transition in the new inflationary universe scenario and generation of perturbations, Phys. Lett. **117B**, 175 (1982).

[8] A. H. Guth and S.-Y. Pi, Fluctuations in the new inflationary universe, Phys. Rev. Lett. **49**, 1110 (1982).

[9] J. M. Bardeen, P. J. Steinhardt, and M. S. Turner, Spontaneous creation of almost scale-free density perturbations in an inflationary universe, Phys. Rev. D **28**, 679 (1983).

[10] N. Aghanim *et al.* (Planck Collaboration), Planck 2018 results—VI. Cosmological parameters, Astron. Astrophys. **641**, A6 (2020).

[11] M. Giovannini, Spikes in the relic graviton background from quintessential inflation, Classical Quantum Gravity **16**, 2905 (1999).

[12] M. Giovannini, Production and detection of relic gravitons in quintessential inflationary models, Phys. Rev. D **60**, 123511 (1999).

[13] M. Giovannini, Low scale quintessential inflation, Phys. Rev. D **67**, 123512 (2003).

[14] G. Cognola, E. Elizalde, S. Nojiri, S. D. Odintsov, L. Sebastiani, and S. Zerbini, Class of viable modified $f(r)$ gravities describing inflation and the onset of accelerated expansion, Phys. Rev. D **77**, 046009 (2008).

[15] R. Myrzakulov, L. Sebastiani, and S. Vagnozzi, Inflation in $f(R,\phi)$—theories and mimetic gravity scenario, Eur. Phys. J. C **75**, 444 (2015).

[16] A. Salvio, Inflationary perturbations in no-scale theories, Eur. Phys. J. C **77**, 267 (2017).

[17] V. K. Oikonomou, Viability of the intermediate inflation scenario with F(T) gravity, Phys. Rev. D **95**, 084023 (2017).

[18] A. Agarwal, R. Myrzakulov, M. Sami, and N. K. Singh, Quintessential inflation in a thawing realization, Phys. Lett. B **770**, 200 (2017).

[19] A. I. Keskin, Viable super inflation scenario from F(T) modified teleparallel gravity, Eur. Phys. J. C **78**, 705 (2018).

[20] A. Salvio, Quasi-conformal models and the early universe, Eur. Phys. J. C **79**, 750 (2019).

[21] S. Castello, S. Ilić, and M. Kunz, Updated dark energy view of inflation, Phys. Rev. D **104**, 023522 (2021).

[22] R. L. Workman *et al.*, Inflation (2023), Prog. Theor. Exp. Phys. **2022**, 083C01 (2022).

[23] A. Achúcarro *et al.*, Inflation: Theory and observations, arXiv:2203.08128.

[24] Y. Akrami *et al.* (Planck Collaboration), Planck 2018 results - X. Constraints on inflation, Astron. Astrophys. **641**, A10 (2020).

[25] W. Giarè, F. Renzi, O. Mena, E. Di Valentino, and A. Melchiorri, Is the Harrison-Zel'Dovich spectrum coming back? ACT preference for $n_s \sim 1$ and its discordance with Planck, Mon. Not. R. Astron. Soc. **521**, 2911 (2023).

[26] E. Di Valentino, W. Giarè, A. Melchiorri, and J. Silk, Health checkup test of the standard cosmological model in view of recent cosmic microwave background anisotropies experiments, Phys. Rev. D **106**, 103506 (2022).

[27] E. Di Valentino, W. Giarè, A. Melchiorri, and J. Silk, Quantifying the global "CMB tension" between the Atacama Cosmology Telescope and the Planck satellite in extended models of cosmology, Mon. Not. R. Astron. Soc. **520**, 210 (2023).

[28] R. Calderon, A. Shafieloo, D. Kumar Hazra, and W. Sohn, On the consistency of λCDM with CMB measurements in light of the latest Planck, ACT and SPT data, J. Cosmol. Astropart. Phys. 08 (2023) 059.

[29] P. Ade *et al.*, Improved constraints on primordial gravitational waves using Planck, WMAP, and BICEP/Keck observations through the 2018 observing season, Phys. Rev. Lett. **127**, 151301 (2021).

[30] P. Campeti and E. Komatsu, New constraint on the tensor-to-scalar ratio from the Planck and BICEP/Keck array data using the profile likelihood, Astrophys. J. **941**, 110 (2022).

[31] P. A. R. Ade *et al.* (Spider Collaboration), A constraint on primordial b-modes from the first flight of the Spider Balloon-borne Telescope, Astrophys. J. **927**, 174 (2022).

[32] N. Arkani–Hamed, S. Dimopoulos, and G. Dvali, The hierarchy problem and new dimensions at a millimeter, Phys. Lett. B **429**, 263 (1998).

[33] L. Randall and R. Sundrum, Large mass hierarchy from a small extra dimension, Phys. Rev. Lett. **83**, 3370 (1999).

[34] L. Randall and R. Sundrum, An alternative to compactification, Phys. Rev. Lett. **83**, 4690 (1999).

[35] G. Dvali, G. Gabadadze, and M. Porrati, 4d gravity on a brane in 5d Minkowski space, Phys. Lett. B **485**, 208 (2000).

[36] N. Deruelle, T. Doležel, and J. Katz, Perturbations of brane worlds, Phys. Rev. D **63**, 083513 (2001).

[37] R. A. Battye, B. Carter, A. Mennim, and J.-P. Uzan, Einstein equations for an asymmetric brane-world, Phys. Rev. D **64**, 124007 (2001).

[38] R. A. Battye and B. Carter, Generic junction conditions in brane-world scenarios, Phys. Lett. B **509**, 331 (2001).

[39] J. Nash, The imbedding problem for Riemannian manifolds, Ann. Math. **63**, 20 (1956).

[40] R. E. Greene, *Isometric Embeddings of Riemannian and Pseudo-Riemannian Manifolds*, Mem. Am. Math. Soc. (1970), Vol. 97, https://bookstore.ams.org/memo-1-97/.

[41] M. Maia and E. M. Monte, Geometry of brane-worlds, Phys. Lett. A **297**, 9 (2002).

[42] M. D. Maia, E. M. Monte, J. M. F. Maia, and J. S. Alcaniz, On the geometry of dark energy, Classical Quantum Gravity **22**, 1623 (2005).

[43] M. D. Maia, N. Silva, and M. C. B. Fernandes, Brane-world quantum gravity, J. High Energy Phys. 04 (2007) 047.

[44] M. D. Maia, A. J. S. Capistrano, J. S. Alcaniz, and E. M. Monte, The deformable universe, Gen. Relativ. Gravit. **43**, 2685 (2011).

[45] M. Heydari-Fard and H. Sepangi, Anisotropic brane gravity with a confining potential, Phys. Lett. B **649**, 1 (2007).

[46] S. Jalalzadeh, M. Mehrnia, and H. R. Sepangi, Classical tests in brane gravity, Classical Quantum Gravity **26**, 155007 (2009).

[47] A. Ranjbar, H. R. Sepangi, and S. Shahidi, Asymptotically Lifshitz brane-world black holes, Ann. Phys. (N.Y.) **327**, 3170 (2012).

[48] A. J. Capistrano, P. T. Seidel, and H. R. Duarte, Subhorizon linear Nash–Greene perturbations with constraints on $H(z)$ and the deceleration parameter $q(z)$, Phys. Dark Universe **31**, 100760 (2021).

[49] A. J. S. Capistrano, L. A. Cabral, J. A. P. F. Marão, and C. H. Coimbra-Araújo, Linear Nash-Greene fluctuations on the evolution of S_8 and H_0 tensions, Eur. Phys. J. C **82**, 1434 (2022).

[50] A. J. S. Capistrano and L. A. Cabral, Effective potential for quintessential inflation driven by extrinsic gravity, Universe **9**, 1 (2023).

[51] W. Israel, Singular hypersurfaces and thin shells in general relativity, Nuovo Cimento B (1965–1970) **44**, 1 (1966).

[52] S. Tsujikawa, M. Sami, and R. Maartens, Observational constraints on braneworld inflation: The effect of a Gauss-Bonnet term, Phys. Rev. D **70**, 063525 (2004).

[53] J. Carron, M. Mirmelstein, and A. Lewis, CMB lensing from Planck PR4 maps, J. Cosmol. Astropart. Phys. 09 (2022) 039.

[54] E. Rosenberg, S. Gratton, and G. Efstathiou, CMB power spectra and cosmological parameters from Planck PR4 with CamSpec, Mon. Not. R. Astron. Soc. **517**, 4620 (2022).

[55] P. A. R. Ade *et al.* (BICEP/Keck Collaboration), Improved constraints on primordial gravitational waves using planck, WMAP, and BICEP/Keck observations through the 2018 observing season, Phys. Rev. Lett. **127**, 151301 (2021).

[56] F. Beutler, C. Blake, M. Colless, D. H. Jones, L. Staveley-Smith, L. Campbell, Q. Parker, W. Saunders, and F. Watson, The 6dF Galaxy Survey: Baryon acoustic oscillations and the local Hubble constant, Mon. Not. R. Astron. Soc. **416**, 3017 (2011).

[57] A. J. Ross, L. Samushia, C. Howlett, W. J. Percival, A. Burden, and M. Manera, The clustering of the SDSS DR7 main Galaxy sample—I. A 4 per cent distance measure at $z = 0.15$, Mon. Not. R. Astron. Soc. **449**, 835 (2015).

[58] S. Alam *et al.* (BOSS Collaboration), The clustering of galaxies in the completed SDSS-III Baryon Oscillation Spectroscopic Survey: Cosmological analysis of the DR12 galaxy sample, Mon. Not. R. Astron. Soc. **470**, 2617 (2017).

[59] Z. Wang, S. H. Mirpoorian, L. Pogosian, A. Silvestri, and G.-B. Zhao, New MGCAMB tests of gravity with CosmoMC and Cobaya, J. Cosmol. Astropart. Phys. 08 (2023) 038.

[60] J. Torrado and A. Lewis, Cobaya: Code for Bayesian analysis of hierarchical physical models, J. Cosmol. Astropart. Phys. 05 (2021) 057.

[61] L. P. Eisenhart, *On Riemannian Geometry* (Dover Publications, New York, 2005).

[62] C. S. Lim, The Higgs particle and higher-dimensional theories, Prog. Theor. Exp. Phys. **2014**, 02A101 (2014).

[63] T. B. Mieling, C. Hilweg, and P. Walther, Measuring spacetime curvature using maximally path-entangled quantum states, Phys. Rev. A **106**, L031701 (2022).

[64] S. Feng, B.-M. Gu, and F.-W. Shu, Quantum gravity induced entanglement of masses with extra dimensions, Eur. Phys. J. C **84**, 59 (2024).

[65] S. N. Gupta, Gravitation and electromagnetism, Phys. Rev. **96**, 1683 (1954).

[66] C. J. Isham, A. Salam, and J. Strathdee, f-dominance of gravity, Phys. Rev. D **3**, 867 (1971).

[67] D. Sapone and M. Kunz, Fingerprinting dark energy, Phys. Rev. D **80**, 083519 (2009).

[68] R. Arjona, W. Cardona, and S. Nesseris, Unraveling the effective fluid approach for $f(r)$ models in the subhorizon approximation, Phys. Rev. D **99**, 043516 (2019).

[69] L. F. Abbott and M. B. Wise, Constraints on generalized inflationary cosmologies, Nucl. Phys. **B244**, 541 (1984).

[70] F. Lucchin and S. Matarrese, Power law inflation, Phys. Rev. D **32**, 1316 (1985).

[71] P. C. W. Davies and V. Sahni, Quantum gravitational effects near cosmic strings, Classical Quantum Gravity **5**, 1 (1988).

[72] J. Martin, C. Ringeval, and V. Vennin, Encyclopaedia inflationaris, Phys. Dark Universe **5–6**, 75 (2014), Hunt for Dark Matter.

[73] K. Becker, M. Becker, and A. Krause, M-theory inflation from multi M5-brane dynamics, Nucl. Phys. **B715**, 349 (2005).

[74] M. Bennai, H. Chakir, and Z. Sakhi, On inflation potentials in Randall-Sundrum braneworld model, Electron. J. Theor. Phys. **9**, 84 (2006), https://citeseerx.ist.psu.edu/document?repid=rep1&type=pdf&doi=5904c18caf58a89eef70546d9cf11f09dfb4d01a.

[75] M. Tristram *et al.*, Planck constraints on the tensor-to-scalar ratio, Astron. Astrophys. **647**, A128 (2021).

[76] J. S. Alcaniz and F. C. Carvalho, β-exponential inflation, Europhys. Lett. **79**, 39001 (2007).

[77] M. Santos, M. Benetti, J. Alcaniz, F. Brito, and R. Silva, CMB constraints on β-exponential inflationary models, J. Cosmol. Astropart. Phys. 03 (**2018**) 023.

[78] P. A. R. Ade *et al.* (Keck Array and BICEP2 Collaborations), Constraints on primordial gravitational waves using Planck, WMAP, and new BICEP2/Keck observations through the 2015 season, Phys. Rev. Lett. **121**, 221301 (2018).

[79] S. Alam *et al.*, Completed SDSS-IV extended Baryon Oscillation Spectroscopic Survey: Cosmological implications from two decades of spectroscopic surveys at the Apache Point Observatory, Phys. Rev. D **103**, 083533 (2021).

[80] N. Sailer, S.-F. Chen, and M. White, Optical depth to reionization from perturbative 21 cm clustering, J. Cosmol. Astropart. Phys. 10 (2022) 007.